ACS APPLIED MATERIALS & INTERFACES

www.acsami.org

Research Article

Incorporating Flexibility Effects into Metal–Organic Framework Adsorption Simulations Using Different Models

Zhenzi Yu, Dylan M. Anstine, Salah Eddine Boulfelfel, Chenkai Gu, Coray M. Colina, and David S. Sholl*

Cite This: *ACS Appl. Mater. Interfaces* 2021, 13, 61305–61315

Read Online

ACCESS | Metrics & More | Article Recommendations | Supporting Information

ABSTRACT: High-throughput calculations based on molecular simulations to predict the adsorption of molecules inside metal–organic frameworks (MOFs) have become a useful complement to experimental efforts to identify promising adsorbents for chemical separations and storage. For computational convenience, all existing efforts of this kind have relied on simulations in which the MOF is approximated as rigid. In this paper, we use extensive adsorption–relaxation simulations that fully include MOF flexibility effects to explore the validity of the rigid framework approximation. We also examine the accuracy of several approximate methods to incorporate framework flexibility that are more computationally efficient than adsorption–relaxation calculations. We first benchmark various models of MOF flexibility for four MOFs with well-established CO_2 experimental consensus isotherms. We then consider a range of adsorption properties, including Henry's constants, nondilute loadings, and adsorption selectivity, for seven adsorbates in 15 MOFs randomly selected from the CoRE MOF database. Our results indicate that in many MOFs adsorption–relaxation simulations are necessary to make quantitative predictions of adsorption, particularly for adsorption at dilute concentrations, although more standard calculations based on rigid structures can provide useful information. Finally, we investigate whether a correlation exists between the elastic properties of empty MOFs and the importance of including framework flexibility in making accurate predictions of molecular adsorption. Our results did not identify a simple correlation of this type.

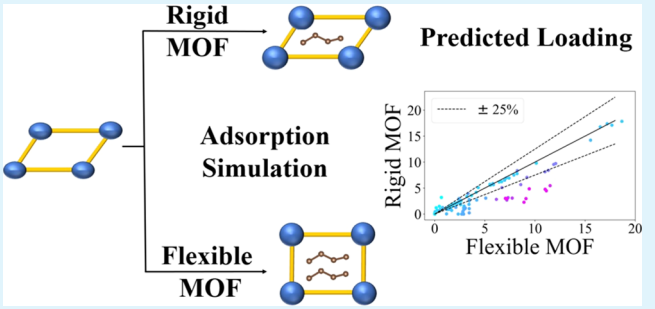

KEYWORDS: *metal–organic frameworks, materials, adsorption, selectivity, flexibility*

INTRODUCTION

Metal–organic frameworks (MOFs) are crystalline nanoporous materials consisting of metal clusters and coordinated organic linkers. These frameworks have been widely studied due to their distinctive features, such as ultrahigh porosities, high surface areas (up to 10 000 m^2/g), and the diverse chemical environments that can be created in their pores.[1−3] Collections of thousands of MOF structures have been systematically developed to enable high-throughput computational studies of MOF properties.[4−7] Multiple studies have used molecular simulation techniques to predict the adsorption properties of molecules in large libraries of MOFs,[7−9] and data of this kind has been used in conjunction with machine learning methods to expand the scope of these predictions.[10−14] To the best of our knowledge, all existing high-throughput studies of adsorption in MOFs are based on molecular simulations in which the MOF structure is assumed to be rigid.

All MOFs exhibit some forms of flexibility, ranging from large-scale structural transformations induced by external stimuli to lattice vibrations around equilibrium positions, which influence adsorption isotherms, selectivity ratios, and intracrystalline diffusivity.[15−17] The different modes of MOF flexibility can be categorized into extrinsic flexibility and intrinsic flexibility. Extrinsic flexibility is triggered by external stimuli and includes MOF swelling, breathing, etc. An instance of MOF extrinsic flexibility that has been carefully described with experiments is MIL-53, which exhibits variations in pore shapes depending on adsorbate loading.[16,18] Another example is Co(BDP), which shows multistage phase transitions during N_2 adsorption.[19] The second flexibility type, intrinsic flexibility, is a ubiquitous phenomenon that occurs due to thermal vibrations of framework atoms, even in the absence of external stimuli. A study by Witman et al. suggested that intrinsic flexibility has significant impacts on molecular adsorption in

Received: October 25, 2021
Accepted: December 7, 2021
Published: December 20, 2021

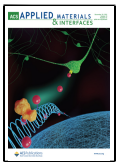

https://doi.org/10.1021/acsami.1c20583
ACS Appl. Mater. Interfaces 2021, 13, 61305−61315

MOFs.[20] Following Witman et al.'s work, Agrawal et al. studied 100 randomly selected structures from the CoRE MOF database[4] and examined the influence of intrinsic flexibility on saturation uptake, Henry's constant, and selectivity.[21]

For MOFs sensitive to flexibility, a variety of models and force fields (FFs) have been developed for incorporating flexibility into adsorption simulations. These models have been previously applied to other materials including polymers and zeolites by combining different ensembles and simulation tools.[22−27] For example, Rogge et al. modeled adsorption in MIL-53 using hybrid Monte Carlo/molecular dynamics (MC/MD) simulations in the osmotic ensemble.[28] This approach allows for influences from adsorbates, temperature, and pressure on MOF flexibility, and thus can capture the phase transition during adsorption. However, it is more difficult to apply than simulations in rigid materials because of the added computational burden. Others tried to simplify the modeling of MOF flexibility using the snapshot method, an approach that neglects adsorbate-induced MOF flexibility and assumes a constant MOF volume.[21,29−32] However, for flexible MOFs, it is not clear a priori which type of flexibility model should be used. Flexible FFs that reproduce experimentally observed structural and adsorption properties of MOFs have been developed,[32] but these FFs are typically system-specific and their transferability is unclear. On the other hand, generic FFs for MOFs have been defined, but their accuracy has only been sparsely tested.

Although techniques are available for modeling flexible MOFs, the trade-off between computational cost and simulation accuracy has led to most work on adsorption in MOFs neglecting flexibility. Inherent in this approach is the assumption that in many cases neglecting flexibility can give results of acceptable accuracy. Being able to reliably identify instances where this is not the case would improve the fidelity of performance predictions from high-throughput simulation approaches.

We focus here on describing the impact of flexibility on adsorption in MOFs using different simulation approaches. In every case, we compare our results to calculations with an adsorption−relaxation method that fully accounts for intrinsic and adsorption-induced framework flexibility. After performing some validation of the generic FF used in our calculations, the UFF4MOF,[33,34] we compare a variety of FF-based simulation methods with consensus isotherms from several well-known MOFs. Some FF-based simulation methods and a FF-free method called the ellipsoid method are then applied to 15 MOFs selected from the CoRE MOF database[4] to illustrate issues that can arise in high-throughput screening. Finally, we explore possible links between the elastic properties of empty MOFs and the influence of MOF flexibility on adsorption.

MODEL AND METHODS

Rigid Adsorption Models. Simulations with rigid MOF structures were performed with methods consistent with earlier studies.[9,35] Two different types of structures are used in the rigid adsorption model: density functional theory (DFT)-optimized structures and FF-relaxed structures. The DFT-optimized structures were energy-minimized using the Perdew−Burke−Ernzerhof (PBE) generalized gradient approximation (GGA) exchange−correlation functional with Becke−Jonson damping D3 dispersion corrections (PBE-D3) using the VASP software. Previous benchmarking calculations have indicated that this approach gives results in good agreement with experimental structures.[36] FF-relaxed structures were energy-minimized using the *cg* style in LAMMPS[37,38] with all degrees of freedom in the MOFs modeled using the UFF4MOF. The stopping tolerance for energy and force was 10^{-10} (kcal/(mol Å)). Simulation input files for LAMMPS were prepared with LAMMPS_INTERFACE and checked manually.[40] We note that UFF4MOF does not include any Coulomb interactions between framework atoms. During the relaxation process in both kinds of calculations, atom positions and the unit cell dimensions were allowed to change.

Single-component adsorption with fixed frameworks was assessed using grand canonical Monte Carlo (GCMC) simulations with RASPA.[39,40] In these GCMC simulations, the van der Waals (vdW) interactions between adsorbates were described by the TraPPE-UA[41,42] FF for hydrocarbons and CO_2. Xe and Kr interaction parameters were taken from the work of Hirschfelder et al.[43] and Talu and Myers,[44] respectively. Lorentz−Berthelot mixing rules were used to define adsorbate−MOF interactions with the vdW parameters for MOF atoms given by the UFF4MOF. Lennard−Jones interactions were truncated at 12 Å with tail energy corrections applied. For polar molecules, Coulombic interactions were modeled pairwise using the long-range Ewald summation scheme with a relative accuracy of 10^{-6}. The point charges on MOF atoms were assigned using the DDEC6 method.[45−47] We reiterate that MOF charges were only used to account for adsorbate−framework interactions in CO_2 adsorption simulations, not within the framework−framework interactions. MOF unit cells were replicated to a minimum of 24 Å along each dimension under triclinic periodic boundary conditions in all dimensions. Monte Carlo trial moves allowing for translation, rotation, reinsertion, deletion, and insertion moves were attempted with equal probabilities during GCMC. Widom insertion was used to compute Henry's constants. 10^5 equilibration and 10^5 production cycles were used in Widom insertion and GCMC simulations, and initial tests indicated this choice gave well-converged results.

Adsorption−Relaxation Flexible Adsorption Models. Adsorption−relaxation simulations were performed at 300 K with a combined GCMC and MD technique using a LAMMPS−RASPA interface developed by Anstine et al.[26] Adsorption−relaxation is carried out in multiple iterations, where GCMC simulations are used to predict adsorbate loading and isothermal−isobaric MD simulations are employed to account for system rearrangement. Each GCMC portion of the adsorption−relaxation approach was performed using RASPA for 10^5 equilibration and production cycles, with the same settings as in the adsorption simulations defined above. MD simulations were carried out with the LAMMPS software package for 1 ns (with a 1 fs timestep) with barostat conditions corresponding to the adsorbate's bulk phase pressure and thermostat conditions corresponding to isotherm temperature. The barostat and thermostat coupling constants were both 0.1 ps. This iterative process was repeated until an equilibrated simulation cell volume and adsorbate loading is reached, which typically required around 10 iterations depending on the structure. The results from the final iteration are regarded as the adsorption properties predicted by the adsorption−relaxation model. These adsorption−relaxation calculations include all effects due to intrinsic and adsorbate-induced flexibility in the MOF. The use of relatively long-time MD simulations to include the influence of structural flexibility is more robust than an alternative such as hybrid MC simulations, which rely on extremely short MD trajectories using time steps chosen to deliberately violate energy conservation.[48] While adsorption−relaxation calculations can be viewed as the "gold standard" for predicting adsorption properties, their computational expense limits high-throughput calculations with diverse collections of adsorbing molecules because independent calculations must be performed for each state point of interest.

Flexible Snapshot Adsorption Models. The snapshot method is an approximate approach for assessing the impact of thermally driven flexibility in an empty MOF structure without the inclusion of adsorbate-induced deformation.[21,29−32] We tested two versions of this method that differ by using either the NVT or NPT ensemble to generate the empty structure's snapshots. These calculations began with FF-relaxed MOF structures defined above and used either NVT or NPT MD simulations at 300 K to account for framework flexibility. The temperature in these simulations was controlled using the Nosé−

https://doi.org/10.1021/acsami.1c20583
ACS Appl. Mater. Interfaces 2021, 13, 61305−61315

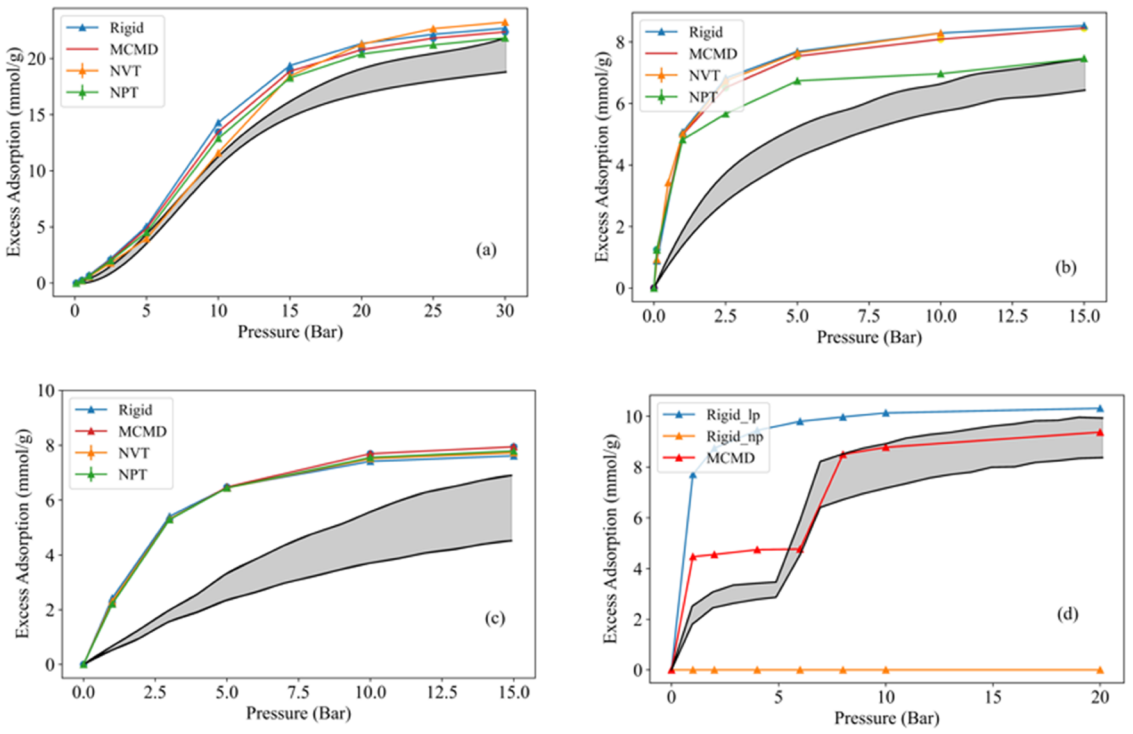

Figure 1. CO_2 adsorption isotherms in (a) IRMOF-1, (b) UiO-66, (c) ZIF-8, and (d) MIL-53 (lp: large pore, np: small pore). Symbols and lines show simulation results at 300 K using the methods described in the text, and shaded regions represent the upper and lower quartiles from experimental consensus isotherm reported by Park et al.[57] at 298 ± 5 K.

Hoover thermostat with a decay period of 0.1 ps. A barostat is used to maintain a pressure of 10 bar in the NPT snapshot flexible model with a decay period of 0.1 ps. MD simulations were performed with a timestep of 1 fs for an equilibration period of 500 ps and a production period of 1 ns. Flexible snapshots from our MD simulations were taken every 100 ps from the production period for a total of 10 snapshots, which was shown previously to give adequately converged results for MOFs.[21] Following this process, each snapshot was treated as rigid and GCMC simulations in each snapshot were conducted using the techniques described above. Reported loadings are averaged over the independent snapshots. Although the snapshot method is more computationally demanding than calculations based on rigid structures, it is amenable to high-throughput calculations because the set of snapshots for each material is independent of the adsorbing species or mixture.

Ellipsoid Model. A disadvantage of the flexible snapshot methods and adsorption−relaxation approaches is that they rely on the availability of high-quality force fields for the framework degrees of freedom. It would be helpful to have approximate means to determine the importance of framework flexibility for new materials without invoking an FF. Below, we explore an FF-free approach based on the observation that when MOF crystal structures are obtained experimentally from single-crystal data atomic vibration parameters, also known as thermal parameters, are reported alongside the locations of atoms. These parameters are readily available in Crystallographic Information Files (CIF)[49] for MOFs and many other crystalline materials, and they give a direct quantitative description of the displacements in a MOF structure due to thermal vibrations.[50,51] Our ellipsoid method generates physically plausible snapshots of a flexible MOF using these experimentally measured atomic displacement parameters instead of using FF-based MD.

Atomic displacement parameters from experimental structures are typically reported only for nonhydrogen atoms and are either provided in an isotropic or anisotropic form, denoted as a single value U_{equiv} or a 3 × 3 matrix with elements U_{ij}, respectively. We, therefore, use U_{equiv} as the variance for a Gaussian distribution or use the matrix elements U_{ij} as covariances for a multivariate Gaussian distribution to estimate nonhydrogen atom displacements. These parameters are rescaled from the experimental temperature to the temperature of interest by reweighting using a Boltzmann factor. Snapshots were generated by sampling the Gaussian distributions of atomic positions for nonhydrogen atoms and fixing hydrogen atoms bonded to heavy atoms at the relative positions defined in the experimentally reported structure. Initial tests with this approach showed that moving each heavy atom in an uncorrelated way led to unphysical bond lengths and, as a result, to physically implausible structures. To avoid unphysical bond length changes, correlations are added between bonded atoms, which means the final vibration of an atom is the average of the Gaussian displacement from itself and its bonded atoms. For example, for a Zn atom coordinated by four oxygen atoms, the displacement of the Zn atom is calculated as $0.5 \times Vib_{zn} + 0.5 \times \text{avg}(Vib_{Ox})$, where Vib_{zn} and Vib_{Ox} represent the uncorrelated displacement of the Zn atom and the coordinated oxygen atoms, respectively. Once a set of independent structures have been generated with this approach, the adsorption properties of each structure are assessed using GCMC in the same way as in the flexible snapshot method. As with the snapshot method, the ellipsoid method includes information about the constant volume flexibility of the empty structure but not any effects associated with adsorption-induced deformation.

The method defined above can be readily applied when an experimental crystal structure is available. We acknowledge there are numerous examples where this experimental data is not available, including disordered porous materials and hypothetical porous materials generated from computational approaches.[52] For these cases, the ellipsoid method could still be applied using Gaussian parameters that are adapted from similar materials.

Computational Overhead for Approximate Methods and Adsorption−Relaxation Calculations. It is useful to consider the relative computational time associated with the various methods defined above. Here, we give expressions for the computational time associated with predicting the single-component adsorption of N_{ads} different adsorbates at N_P different pressure values in a single MOF in calculations where the time for a GCMC calculation in a given rigid

https://doi.org/10.1021/acsami.1c20583
ACS Appl. Mater. Interfaces 2021, 13, 61305−61315

structure is t_{GCMC} and the time for an MD simulation of the same MOF is t_{MD}. The ratio t_{GCMC}/t_{MD} depends on a variety of factors that may differ between computing environments. For example, in our calculations, MD was performed with a code that is readily run in parallel, an advantage not available in GCMC. If multiple GCMC simulations are performed within a single rigid structure, then it is advantageous to precompute the adsorbate's potential energy on a finely space grid, but this effort may be less worthwhile in adsorption−relaxation calculations where a completely new grid is necessary for every GCMC calculation. We have not attempted to include the effects of these grids in the following estimates of timing.

The computational time required for a single MOF using rigid structure calculations as defined above is $t_{rigid} = N_p N_{ads} t_{GCMC}$. The time necessary for the same MOF using the snapshot method is $t_{snapshot} = N_{snapshot}(t_{rigid} + t_{MD})$, where $N_{snapshot}$ is the number of independent snapshots used. If calculations are performed for a sizeable number of pressure points and/or different adsorbates, then the MD contribution to this time is negligible, so $t_{snapshot}$ is approximately $N_{snapshot}\ t_{rigid}$. For adsorption−relaxation calculations, the time required is $t_{ads\text{-}rel} = N_{it} t_{rigid}(1 + t_{MD}/t_{GCMC})$, where N_{it} is the number of adsorption−relaxation iterations needed to reach convergence. It is evident from this expression that if adsorption−relaxation calculations were going to be attempted for large collections of materials, then it would be valuable to understand how to minimize t_{MD}/t_{GCMC} and N_{it} while still achieving well-converged results.

Calculation of Geometrical Properties. We characterized the internal void of each MOF by computing what Ongari et al. termed the probe-accessible and probe-occupiable pore volume using the Zeo ++ code version 0.3.31.[53,54] The total accessible void fraction is the sum of these two quantities. We calculated the accessible void fraction using He as the probe with a radius of 1.32 Å.[54]

Calculation of Elastic Properties. The elastic properties of empty MOFs, including the bulk, shear, and Young's moduli, were calculated by determining the elastic tensor at 0 K. We used a similar method to that in the calculations for multiple MOFs by Rogge et al.[55] The elastic tensors were obtained by least-squares linear fit of $\sigma = C\epsilon$. Four pairs of data were obtained by the application of a modest compressive and elongational constant strain ($\epsilon = \pm 0.005, \pm 0.01$) in six independent directions and remapping atomic coordinates to the deformed simulation cell before relaxation. The methods for energy minimization, application of periodic boundary conditions, and convergence criteria were the same as in the work of Rogge et al. The accuracy of FF-based calculations of this tensor with UFF4MOF has previously been validated by comparing to results from an ab initio-derived FF by Moghadam et al.[56]

RESULTS AND DISCUSSION

Benchmarking with Experimental Data. We initially selected four MOFs with well-established consensus isotherms for room-temperature CO_2 adsorption for our benchmark: IRMOF-1, UiO-66, ZIF-8, and MIL-53. Experimental consensus isotherms were obtained from a literature meta-analysis conducted by Park et al.[57] These materials are among the most widely studied of all MOFs.[58] UFF4MOF gave optimized structures for each of these materials in good agreement with DFT-optimized structures and with experimental data (see Supporting Information Table S1). This observation suggests that UFF4MOF is an appropriate FF for each material.

Simulated isotherms were obtained from each of the rigid and flexible models defined above. These results are compared to the consensus experimental data in Figure 1. For IRMOF-1, ZIF-8, and UiO-66, the adsorption−relaxation calculations and the rigid structure calculations give isotherms that differ only marginally. Not surprisingly, the two variants of the snapshot method are also consistent with these results in IRMOF-1 and ZIF-8. Notably, some systematic difference exists between the simulated and experimental data for IRMOF-1, ZIF-8, and UiO-66; this observation was also noted in the work of Park et al. for simulations with the rigid structures.[57] Our calculations show that this difference is not due to a neglect of framework flexibility. Instead, our results point to the generic FF used to describe the adsorbates as not being quantitatively accurate. The CO_2 adsorption results for IRMOF-1 and ZIF-8 are examples where using the more computationally demanding adsorption−relaxation method does not lead to results that differ in any significant way from the simpler rigid structure calculations.

In UiO-66, the NPT snapshot method gives a lower uptake than the other methods due to the large negative thermal expansion (NTE) predicted by the simulations. This strong NTE is not consistent with experimental observations of the UiO-66 structure and appears to be caused by inaccuracy of the UFF4MOF. More information on this issue is given in the Supporting Information. The UFF4MOF predicts negligible thermal expansion for ZIF-8 and IRMOF-1, so the NPT and NVT snapshot method results for these two materials are similar.

MIL-53 is different from the three examples discussed above because it is known to undergo adsorption-induced phase transitions together with large cell volume changes. Figure 1d shows GCMC results from two different rigid structures, a large pore (lp) structure and a narrow pore (np) structure.[28] In situations like this, simulations using the osmotic ensemble can be used to predict when a transition between the rigid structures will occur.[59,60] Figure 1d shows that the results from our adsorption−relaxation calculations can capture the two steps observed in the experimental isotherms based on a single initial structure, namely, MIL-53-lp, without using the osmotic ensemble. This observation is useful because it did not require prior knowledge or assumptions about the possible structures available to the MOF, which are required by the osmotic ensemble. As with the other three MOFs there are some systematic deviations between the loadings predicted by our calculations and the consensus experimental data, suggesting that the FF used to describe the adsorbate−framework interactions is not quantitatively accurate. It is clear from Figure 1d that the MOF's volume depends on the CO_2 pressure. The predicted trends in this volume as a function of pressure are shown in Figure S5.

Flexibility Effects on Adsorption at High Loading Conditions for a Diverse Range of MOFs. The results above for CO_2 in IRMOF-1, UiO-66, ZIF-8, and MIL-53 are examples in which the only significant effect from structure flexibility is in a material that was previously known to undergo an adsorbate-induced phase transition. Previous calculations using the snapshot method for a wider range of MOFs, however, have suggested that framework flexibility even in the absence of adsorbate-induced changes can have a strong impact on adsorption properties in MOFs.[21] For high-throughput calculations to accurately predict adsorption in MOFs, it would be useful to understand what kinds of structures exhibit flexibility effects that cannot be neglected. To begin to examine this issue, we performed calculations for a set of 15 MOFs selected randomly from the subset of the CoRE MOF database whose room-temperature Henry's constants for butane, using rigid models, are greater than 10^{-5} mol/(m^3·Pa). The structure codes for these materials, along with their cell parameters obtained from DFT calculations and FF

https://doi.org/10.1021/acsami.1c20583
ACS Appl. Mater. Interfaces 2021, 13, 61305−61315

optimization are listed in Table S2. The UFF4MOF gives accurate cell parameter predictions with a mean absolute difference of 2.4% compared to DFT-optimized structures. Because of the computational demands of these calculations, applying the same methods to the large numbers (thousands) of distinct structures sometimes examined in high-throughput calculations with rigid structures would be challenging.

For each MOF, we computed the room-temperature single-component adsorption of seven molecules (ethene, ethane, propene, propane, butane, Xe, and Kr) at a pressure of 10 bar. Figure 2 compares the loading for each example determined

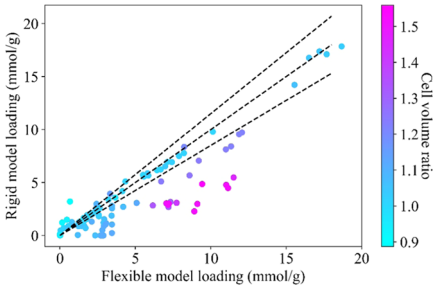

Figure 2. Comparison between loading at room temperature and a pressure of 10 bar for seven molecules (ethene, ethane, propene, propane, butane, Xe, and Kr) in 15 MOFs as predicted by fully flexible calculations (with the adsorption−relaxation model) and with rigid FF-optimized MOF structures. The color bar shows the ratio of cell volume in the flexible structure and the rigid structure. Exact values are listed in the adsorbate.csv files in the SI. Dotted lines show a parity line and values deviating from the parity line by ±25%.

with the adsorption−relaxation method to the loading obtained using the rigid FF-optimized structures. Among the 105 data points in Figure 2, 47.6% have loadings that changed by less than 25% ($|\log(q_{flex}/q_{rigid})| < 0.1$) upon including flexibility, 41.9% had loadings that were underestimated by 25% or more in the rigid structure, and 10.4% had loadings in the rigid structure that were overestimated by 25% or more. The distribution of $\log(q_{flex}/q_{rigid})$, where q is the loading at 10 bar, has a shape close to Gaussian distribution. The mean (μ) and standard deviation (σ) of this distribution are 0.13 and 0.60, respectively (see Figure S10). Both μ and σ are larger than the results from the work of Agrawal et al. using the NVT snapshot method[21] ($\mu = -0.02$, $\sigma = 0.06$), indicating the flexibility has a stronger impact on adsorption than was estimated in previous work.

Many of the cases in which the rigid structure underestimates the loading are associated with swelling of the structure upon adsorption, as shown by the color bar in Figure 2. A striking example of this effect is the MOF AROFET, for which adsorption of the seven adsorbates listed above increases the unit cell volume by around 48%. Notably, the change in volume from temperature and pressure alone for this material is −3%, which means that adsorbates have the dominant impact on swelling. AROFET structures obtained from different models are shown in Figure S7, showing that the MOF swelling occurs via the extension of the originally bent ligand.

Although the unit cell volume is a convenient measure of swelling, a more relevant quantity for adsorption is the accessible volume. The accessible volume of flexible structures was obtained by removing the adsorbed molecules from the structures in equilibrated adsorption−relaxation calculations. The change for the accessible volume is often larger than the comparable effect for the unit cell volume, as it contains the influence of both unit cell and pore environment. Figure S6 compares loadings in fully flexible and rigid structures in terms of the ratio of the accessible volume in the two structures. There are several MOFs in which the accessible volume in the rigid structure is small but for which significant adsorbed loadings are observed in the flexible material.

It is straightforward to understand how swelling of a MOF can lead to calculations with rigid structure underestimating adsorption loadings. There are examples in Figure 2, however, where there is negligible swelling of structures and the fully flexible results give lower loadings than the rigid structures. For example, in GITWIQ, the computed loading of butane is 1.79 mmol/g in the flexible structure, compared to 1.91 mmol/g in the rigid structure, while the volume ratio of the two structures is 1.02. Temperature and pressure alone change the volume of this MOF by −1%, and the adsorbate slightly enlarges the volume by 3%. Images of these two structures are shown in Figure S8, where it can be seen that local disorder and rotation in the MOF's linkers reduce the accessible surface area in the flexible material. This effect can be captured quite accurately by calculations with the NVT snapshot method; for this example, the NVT snapshot model gives a loading of 1.74 mmol/g. A similar phenomenon has also been observed by Anstine et al., where local structure change occurs to a greater extent than macroscopic volume change in microporous polymers.[26]

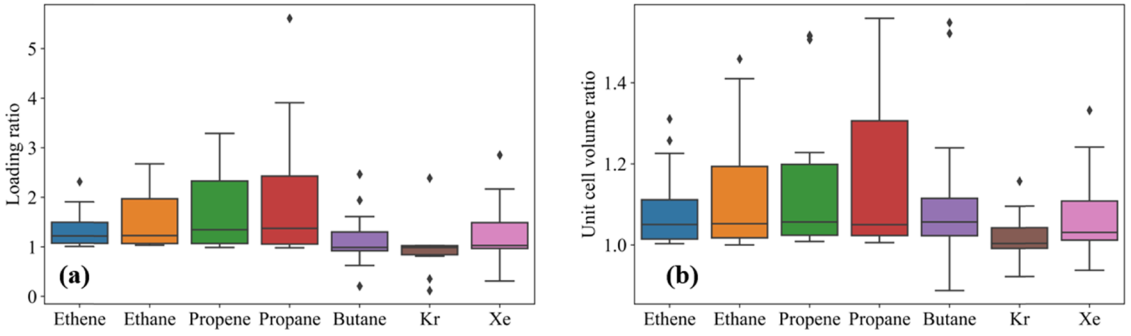

Figure 3. (a) Ratio of loadings between the adsorption−relaxation model and rigid FF-optimized model for individual species in 15 MOFs at room temperature and 10 bar. (b) Ratio unit cell volume comparison from the same calculations. Boxes show the quartiles of the dataset, while whiskers extend to show the rest of the distribution, except for points that are determined to be outliers. Outliers are defined as values more than 1.5IQR (IQR = interquartile range) from either end of the box.[61]

https://doi.org/10.1021/acsami.1c20583
ACS Appl. Mater. Interfaces 2021, 13, 61305−61315

The impact of flexibility on the adsorption loadings of different adsorbates at a pressure of 10 bar is summarized in Figure 3. In general, the degree of swelling increases as the molecular weight of the adsorbate increases. Butane appears to be an exception to this trend, but this is because butane is too large to have a significant loading in some of our simulated MOFs and thus no adsorbate-induced swelling can happen. For example, CUNWEO has a 50% unit cell volume expansion with a 7.0 mmol/g uptake of propane but less than 10% unit cell volume shrinkage with 0.6 mmol/g butane uptake. If only the MOFs that can adsorb 1.5 mmol/g or more of butane are included, then the loading and volume change for butane are larger than our results for C_2 and C_3 hydrocarbons, as shown in Figure S9.

Flexibility Effects on Adsorption at Dilute Loadings for a Diverse Range of MOFs. Previous work by Witman et al.,[20] Agrawal et al.,[21] and Park et al.[29] indicated that intrinsic flexibility of MOFs can cause considerable sensitivity in the determination of Henry's constants. It is useful to look at this issue for the same set of 15 MOFs and 7 adsorbates that we considered above. The adsorption−relaxation and NPT snapshot models yield equivalent results at dilute loadings, as adsorbate-induced framework rearrangement is minimal in this limit. Thus, structures from the NPT snapshot model at 300 K, 1 bar are used to calculate Henry's constant here. These structures are influenced by both intrinsic flexibility and thermally driven volume changes, while in the previously mentioned studies, only the effect of intrinsic flexibility was considered.

Henry's constants obtained from flexible and rigid MOF calculations are shown in Figure 4. Among the 105 cases in

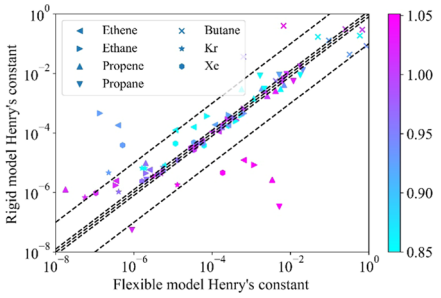

Figure 4. Comparison between Henry's constant (mol/(m^3·Pa)) of 7 adsorbates in 15 MOFs predicted by the flexible model and rigid model. The flexible model here refers to the NPT snapshot model and the rigid model used FF-minimized structures. The color bar represents the unit cell volume ratio of flexible structure to the rigid structure, which is limited to 0.85−1.05 for visualization purposes; exact values are listed in the SI. The inclined dashed lines mark $|\log(Kh_{flex}/Kh_{rigid})| = 0.1$ and 1, respectively.

Figure 4, 16.2% have $|\log(Kh_{flex}/Kh_{rigid})|$ less than 0.1 (which means that the change in Henry's constants due to flexibility is less than ∼25%), 40.9% have $|\log(Kh_{flex}/Kh_{rigid})|$ between 0.1 to 1, and 42.8% have $|\log(Kh_{flex}/Kh_{rigid})|$ larger than 1. The distribution of $\log(Kh_{flex}/Kh_{rigid})$ is close to a Gaussian distribution with $\mu = -0.25$ and $\sigma = 0.77$ (see Figure S11). Compared to the results from Agrawal et al. using the NVT snapshot method[21] ($\mu = 0.38$, $\sigma = 1.11$), the flexibility has a similar influence on these 105 cases, but with a tendency to reduce the Henry's constant relative to the rigid simulations. This is because some MOFs are predicted to have unit cell volume changes due to NTE at dilute loadings. For example, UFF4MOF predicts COGWEB experiences an ∼ 20% volume decrease due to NTE, and all Henry's constants calculated in this MOF are strongly affected. Usually, we observe that NTE is caused by bond length changes, especially near metal clusters. We note by comparison with the NTE discussed above for UiO-66 that the accuracy of the UFF4MOF in instances with large NTE is unclear. Henry's constants in MOFs without a large unit cell volume change can still be influenced by significant flexibility effects when their accessible volume is small. One example is FIPXEJ, whose fraction of accessible volume is the smallest among the 15 MOFs. It has a 12.4% change in inaccessible volume when flexibility is included, but this leads to a drastic change of more than 1100% in the ethene Henry's constant.

The impact of flexibility on Henry's constants increases with increasing adsorbate size (kinetic diameter). The median values of $|\log(Kh_{flex}/Kh_{rigid})|$ for Kr (kinetic diameter d = 3.60 Å[62]), Xe (3.96 Å[62]), ethene (4.16 Å[63]), ethane (4.44 Å[63]), propane (4.30 Å[64]), propene (4.50 Å[64]), and butane (4.68 Å[65]) are 0.26, 0.31, 0.39, 0.42, 0.46, 0.51, and 1.61, respectively. It is also interesting to ask whether the impact of flexibility on Henry's constants is correlated among different molecules. The Pearson product−moment correlation coefficients of Henry's constants in Figure 5 show that Henry's constants of adsorbates with similar geometry are highly correlated, while adsorbates with different geometry are less correlated.

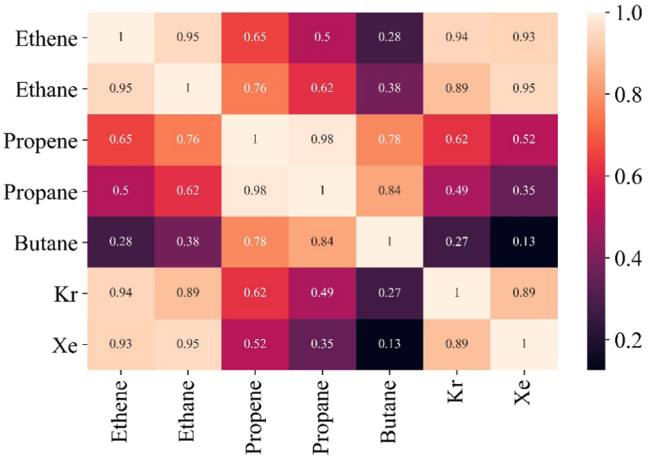

Figure 5. Pearson product−moment correlation coefficients of Henry's constants between different adsorbate pairs at 300 K.

The ratio of Henry's constants for two molecules is, without approximation, the adsorption selectivity for a mixture of these molecules in the dilute limit.[66] In Figure 6, we show the selectivity for 21 pairs of adsorbates (all of the pairs that can be formed between the 7 adsorbates we simulated) in 15 MOFs. The shaded regions in Figure 6 indicate cases where including flexibility changes which species the MOF is predicted to selectively adsorb. Only 10 examples fall into this category, but considerable scatter around the parity line can be seen. The distribution of $\log(S_{flex}/S_{rigid})$ is shown in Figure S12, giving $\mu = -0.02$ and $\sigma = 0.80$. The deviation in our study is slightly larger than the results from Agrawal et al.[21] ($\mu = -0.01$, $\sigma = 0.57$). Based on the comparison between the distribution of selectivity and Henry's constants, the effects of flexibility partially cancel out in mixtures with similar geometry, e.g.,

https://doi.org/10.1021/acsami.1c20583
ACS Appl. Mater. Interfaces 2021, 13, 61305−61315

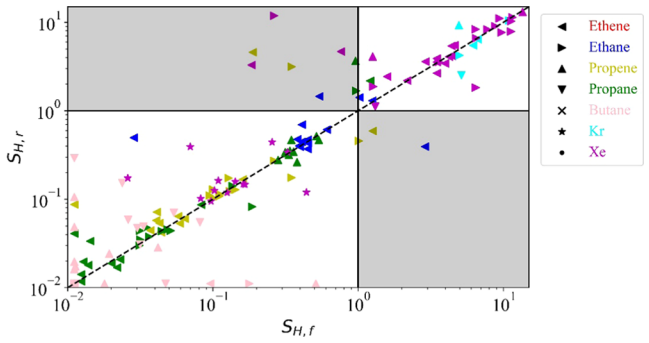

Figure 6. Dilute loading mixture selectivity at 300 K calculated using the NPT flexible model (horizontal axis) and rigid model (vertical axis). For visualization purposes, selectivity values <0.01 are shown as 0.01. Shapes and colors represent the A/B mixture pair with the adsorbate represented by the shape being A and the adsorbate represented by the color being B. For example, the red dot indicates the selectivity of Xe (circle) to ethene (red color).

ethene/ethane, but they tend to be uncorrelated (and therefore stronger) for mixtures with different geometries, e.g., ethene/butane. Therefore, mixtures of dissimilar molecules are most likely to be misrepresented with a rigid framework approximation because flexibility effects are compounded rather than being offset.

Comparison between Approximate Simulations and Adsorption−Relaxation Simulations. Although adsorption−relaxation simulations are a reliable strategy to fully include the effects of MOF flexibility in simulating adsorption, they are not well suited to high-throughput calculations. It is therefore worthwhile to explore criteria for appropriately choosing to apply the thorough adsorption−relaxation technique or a computationally efficient alternative.

A qualitative way to consider each approximate method is to ask whether the method can predict the relative ranking of MOFs in terms of species loading. This issue is probed by Spearman's correlation coefficients, which is a nonparametric measure of rank correlation. Spearman's correlation coefficients comparing the ranking of MOFs in terms of their loading at 10 bar given by approximate methods and the fully flexible simulations are shown in Figure S14. In each case, Spearman's coefficients for different molecules are similar. Spearman's coefficients for the simulations with rigid structures (the most widely used and computationally efficient approximate method) and the flexible snapshot approach with either NVT structures or the ellipsoid approach are all >0.8, indicating a high degree of correlation. Somewhat surprisingly, the flexible snapshot method with NPT structures performs considerably worse, with Spearman's coefficients as low as ∼0.2.

Figure 7 compares the predicted adsorption loadings at 10 bar from four approximate simulation methods to predicted loadings from the adsorption−relaxation model. As already noted above, multiple examples exist where each approximate method fails to be quantitatively accurate, although there are also examples where the impact of flexibility is minimal and all of the methods give similar results. Notably, MOFs with close to zero loadings, for example, BENXUP, have extremely large errors, which may be due to numerical issues. All of these observations suggest that while the rigid framework simulations are useful for ranking materials, there may be challenges

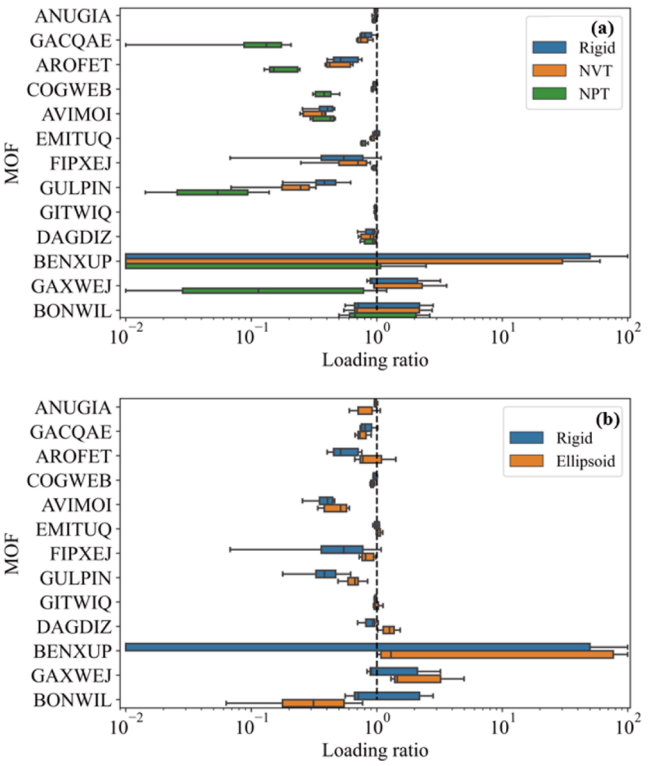

Figure 7. Loading ratio of results from approximate simulations and adsorption−relaxation simulations for seven adsorbates at 10 bar, 300 K. In (a) orange boxes are from the NVT snapshot model, green boxes are from the NPT snapshot model, and blue boxes are from simulations in the rigid FF-optimized structures. In (b), blue boxes are from simulations in rigid FF-optimized structures and orange boxes are from simulations from the ellipsoid model. The box plot uses the same approach as Figure 3, but outlier data points are not shown in this plot. The specific value can be found in adsorbate.csv files in the SI. The MOFs are ordered according to the ethene loading using the adsorption−relaxation model, where ANUGIA has the largest loading.

in using these kinds of simulations to make quantitatively accurate predictions about diverse sets of MOFs.

A comparison between simulations fully accounting for MOF flexibility and approximate methods for Henry's constants is shown in Figure 8. As discussed above, dilute loadings (represented by Henry's constants) are more sensitive

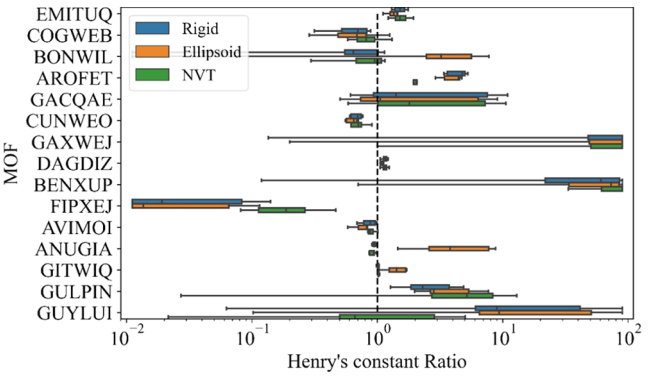

Figure 8. Henry's constant ratios of different approximate simulations to adsorption−relaxation simulations for 7 adsorbates in 15 MOFs. The presentation of the figure is similar to Figure 7.

https://doi.org/10.1021/acsami.1c20583
ACS Appl. Mater. Interfaces 2021, 13, 61305−61315

to MOF flexibility than nondilute adsorption loadings. Spearman's correlation coefficients comparing the ranking of MOFs in terms of their Henry's constants given by approximate methods and the fully flexible simulations are shown in Figure S15. The flexible snapshot method with NVT structures has similar Spearman's coefficients (0.7−0.9) to the results for higher loadings in Figure S14, but simulations with the rigid structures or with the ellipsoid method are quite poorly correlated with the fully flexible simulations, with Spearman's coefficients of 0.3−0.5. Figure 8 compares the predicted Henry's constants with three approximate simulation methods to adsorption−relaxation results. Similar to our discussion above, rigid frameworks can yield qualitatively useful predictions while missing some quantitative insights of adsorption properties.

Rapid Identification of Flexible MOFs Using Elastic Properties. The results above suggest that it would be useful to be able to rapidly identify the subset of MOFs for which flexibility has a limited impact on predictions of adsorption. As an initial test of whether this is possible, we considered the mechanical properties of the MOFs we studied as a potential indicator. The mechanical properties of MOFs have been widely examined.[55,67] Instead of using the full elastic matrix, which can be challenging to interpret, the minimum Young's modulus (MinY) and the anisotropy ratio of the maximum shear modulus to the minimum shear modulus (AniG) have been proposed as scalars indicating MOF softness.[68] In terms of computational cost, the mechanical properties of an empty MOF are inexpensive to compute using FFs. In this work, we use the UFF4MOF to predict mechanical properties, which was benchmarked by comparing results from DFT and UFF4MOF at 0 K for UiO-66 and MIL-53 as shown in Table S3 and Figure S16. Results from these two levels of theory agree with each other qualitatively. As mentioned previously by Moghadam et al., there are some quantitative differences between the FF- and DFT-derived mechanical properties.[56] To simulate adsorption in flexible MOFs using the methods we have considered in this paper, it is the response of the MOF at the FF level to the presence of adsorbates that is important.

Figure 9 compares the ratio of adsorbed loadings at 10 bar, 300 K in adsorption−relaxation simulations and in rigid structures to MinY and AniG for the empty MOFs. This figure includes data for 7 adsorbates in 15 different MOFs. We initially expected that materials with small values of MinY or large values of AniG would be particularly susceptible to adsorption-induced adsorption effects. Our data does not support this idea; Spearman's coefficients between the loading ratio and MinY or AniG are both <0.3. Unfortunately, this initial comparison of MOF mechanical properties and the impact of MOF flexibility on adsorption has not given a straightforward way to rapidly test whether a MOF can reliably be simulated using a rigid structure. We hope, however, that these observations spur additional ideas for addressing this issue.

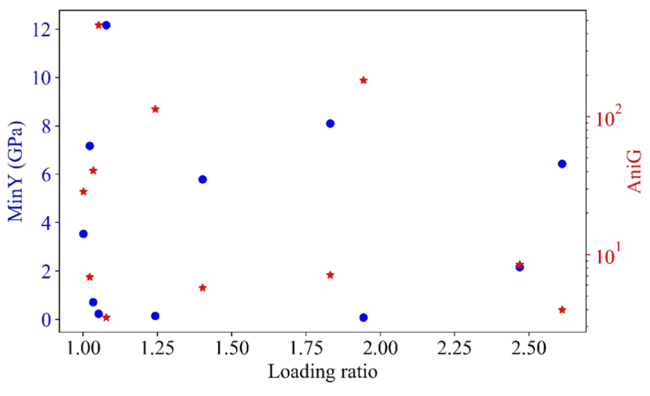

Figure 9. Relationship between loading ratios and mechanical properties of simulated MOFs. The loading ratios are the mean values of the ratios of loadings from the adsorption−relaxation model and loadings from the rigid model at 10 bar, 300 K for seven adsorbates.

CONCLUSIONS

Accurately predicting adsorption properties in MOFs computationally is a useful complement to experimental approaches for identifying high-performing materials for chemical storage or separations. The large number of MOFs and potential adsorbing species that exist have driven strong interest in high-throughput methods for predicting adsorption. To date, all high-throughput molecular simulation efforts for MOFs have utilized a rigid structure approximation. In this paper, we have presented the most comprehensive collection of simulations currently available that fully assess the role of MOF flexibility on adsorption. Our simulations using adsorption−relaxation methods have incorporated all aspects of MOF flexibility during adsorption in a robust way. We presented data for CO_2 adsorption in four well-known MOFs for which consensus experimental isotherms are available and for 7 different adsorbates in 15 MOFs selected randomly from the CoRE MOF database.

Simulated CO_2 adsorption results indicate that the effects of framework flexibility in ZIF-8, IRMOF-1, and UiO-66 are small. For MIL-53 the adsorption−relaxation approach is capable of reproducing the stepped adsorption isotherm shape. This behavior is consistent with the experimentally observed adsorption-induced structural transition. The differences that exist between the isotherms from these calculations and consensus experimental data point to inaccuracies in the force fields used to define adsorbate−MOF interactions. Besides assessing the FF for adsorbate−MOF interactions, we also reported some benchmarking to show UFF4MOF gives accurate predictions for several MOF structures. However, there are cases where intraframework interactions need more testing and careful parameterization. We suggest that future MOF interatomic potentials should consider framework flexibility in their parameterization process, despite the complexities associated with this approach.

For the MOFs selected from the CoRE MOF database, simulations of adsorption of seven different molecules at 10 bar and 300 K showed that including flexibility changes the adsorbed amount by more than 25% in 52% of the cases we considered. In the dilute limit, this effect was stronger, with Henry's constant changing by more than 25% in 84% of cases. In general terms, the effects of flexibility were observed to be strong for larger adsorbates, as might be expected if the outcomes are driven by adsorption-induced effects. The effects of flexibility tend to be similar for similar molecules, so the ideal selectivity calculated from single-component adsorption properties tends to be less sensitive to flexibility for these pairs of molecules. Unfortunately, the same tendency for mixtures of dissimilar molecules is generally not observed. As a result, care should be taken when broadly applying a rigid approximation

https://doi.org/10.1021/acsami.1c20583
ACS Appl. Mater. Interfaces 2021, 13, 61305−61315

method to screen mixture selectivity of diverse species. In this work, we mainly focus on neutral molecules, while the extension of these statements to molecules of differing polarity but similar sizes requires further study.

The adsorption−relaxation model considers the influence of temperature, pressure, and adsorbate on framework flexibility and thus is the most accurate model in our work. However, adsorption−relaxation is a computationally demanding technique and it is therefore worthwhile to consider efficient alternatives and the conditions under which they apply. We assessed the use of approximate models that neglect various factors of framework flexibility. The NVT snapshot and rigid models showed qualitative agreement with adsorption−relaxation data when predicting Henry's constants, but all of the approximate models we tested had limited success in making quantitatively accurate predictions of Henry's constants and loadings under nondilute conditions. When characterized by Spearman's coefficients, the NVT snapshot method is more reliable than more standard rigid structure calculations. These conclusions have important implications for any effort using high-throughput calculations to make predictions about adsorption in MOFs. It would certainly be valuable to develop computationally efficient methods that incorporate the effects of MOF flexibility with greater quantitative reliability than the methods we have tested. In the absence of these methods, it is advisable for high-throughput calculations to be coupled with more detailed adsorption−relaxation calculations for materials of particular interest.

An important observation from our results is that the importance of framework flexibility to accurately describe adsorption in MOFs is difficult to discern before testing. Examples exist for which the impact of framework flexibility is small, so calculations with rigid structures for these structures are reasonably appropriate. At the same time, several systems show large differences between fully flexible calculations and approximate calculations with rigid structures. This situation creates an obvious challenge for accurate high-throughput screening of MOFs as adsorbents. It would be useful if computational characterization methods were available that could categorize MOFs in terms of the degree that framework flexibility impacts adsorption properties. We tested the viability of adsorbate-free MOF elastic properties for addressing this issue. Unfortunately, the correlation between these mechanical properties and the importance of framework flexibility was poor.

Our results illustrate how robust adsorption−relaxation calculations can be used to examine the effects of framework flexibility on adsorption in MOFs. Although these calculations are best suited for detailed studies of individual materials and limited sets of adsorbates, they are less suitable for high-throughput screening because independent calculations must be performed for every state point of interest. To the best of our knowledge, all machine learning models to date aiming to predict adsorption properties of MOFs have been trained on simulation data from rigid structures. Examples exist in which information from one (or a small number of molecules) is used to enable predictions for a range of other adsorbing molecules.[69,70] Thus, one interesting direction for future work may be to augment the training data for machine learning models with carefully selected adsorption−relaxation simulation to capture the impacts of framework flexibility.

■ ASSOCIATED CONTENT

Supporting Information

The Supporting Information is available free of charge at https://pubs.acs.org/doi/10.1021/acsami.1c20583.

Force field validation; examples of structure changes during adsorption; histogram of flexible results compared to rigid results; detailed model comparison figures; MOF mechanical properties of benchmarking MOFs; and link to ellipsoid and adsorption−relaxation model implementation (simulation inputs) (PDF)

Simulated loadings of seven adsorbates at 10 bar, 300 K in Figure 2; simulated Henry's constants of seven adsorbates at 300 K in Figure 4; simulated loadings of using intraframework Coulombic interaction in Figure S4; and full elastic properties for 15 MOFs (ZIP)

■ AUTHOR INFORMATION

Corresponding Author

David S. Sholl − *School of Chemical & Biomolecular Engineering, Georgia Institute of Technology, Atlanta, Georgia 30318, United States; Transformational Decarbonization Initiative, Oak Ridge National Laboratory, Oak Ridge, Tennessee 37830, United States;* orcid.org/0000-0002-2771-9168; Phone: 1-4048942822; Email: david.sholl@chbe.gatech.edu

Authors

Zhenzi Yu − *School of Chemical & Biomolecular Engineering, Georgia Institute of Technology, Atlanta, Georgia 30318, United States*

Dylan M. Anstine − *Department of Materials Science and Engineering, University of Florida, Gainesville, Florida 32611, United States; George and Josephine Butler Polymer Research Laboratory, University of Florida, Gainesville, Florida 32611, United States*

Salah Eddine Boulfelfel − *School of Chemical & Biomolecular Engineering, Georgia Institute of Technology, Atlanta, Georgia 30318, United States*

Chenkai Gu − *School of Chemical & Biomolecular Engineering, Georgia Institute of Technology, Atlanta, Georgia 30318, United States; State Key Laboratory of Coal Combustion and School of Energy and Power Engineering, Huazhong University of Science and Technology, Wuhan, Hubei 430074, China*

Coray M. Colina − *Department of Materials Science and Engineering, University of Florida, Gainesville, Florida 32611, United States; George and Josephine Butler Polymer Research Laboratory, University of Florida, Gainesville, Florida 32611, United States; Department of Chemistry, University of Florida, Gainesville, Florida 32603, United States;* orcid.org/0000-0003-2367-1352

Complete contact information is available at: https://pubs.acs.org/10.1021/acsami.1c20583

Notes

The authors declare no competing financial interest.

■ ACKNOWLEDGMENTS

Z.Y. and D.S.S. received support from the Center for Understanding and Control of Acid Gas-Induced Evolution of Materials for Energy (UNCAGE-ME), an Energy Frontier Research Center funded by the U.S. Department of Energy,

Office of Science, Office of Basic Energy Sciences, under Award No. DE-SC0012577. C.G. received support from the Fundamental Research Funds for the Central Universities (2019kfyRCPY021), China Scholarship Council (201906160014). D.M.A., C.M.C., and D.S.S. received support from the U.S. Department of Energy (DOE), Office of Basic Energy Sciences, Division of Chemical Sciences, Geosciences, and Biosciences under award DE-FG02-17ER16362. The authors thank Hanjun Fang and Raghuram Thyagarajan for technical help and useful discussions.

■ ABBREVIATIONS USED

FF, force field
MOF, metal−organic framework
MinY, minimum Young's modulus
AniG, anisotropy ratio of the maximum shear modulus to the minimum shear modulus

■ REFERENCES

(1) Farha, O. K.; Eryazici, I.; Jeong, N. C.; Hauser, B. G.; Wilmer, C. E.; Sarjeant, A. A.; Snurr, R. Q.; Nguyen, S. T.; Yazaydın, A. Ö.; Hupp, J. T. Metal−Organic Framework Materials with Ultrahigh Surface Areas: Is the Sky the Limit? *J. Am. Chem. Soc.* **2012**, *134*, 15016−15021.
(2) Xuan, W.; Zhu, C.; Liu, Y.; Cui, Y. Mesoporous Metal−Organic Framework Materials. *Chem. Soc. Rev.* **2012**, *41*, 1677−1695.
(3) Furukawa, H.; Cordova, K. E.; O'Keeffe, M.; Yaghi, O. M. The Chemistry and Applications of Metal-Organic Frameworks. *Science* **2013**, *341*, No. 1230444.
(4) Chung, Y. G.; Haldoupis, E.; Bucior, B. J.; Haranczyk, M.; Lee, S.; Zhang, H.; Vogiatzis, K. D.; Milisavljevic, M.; Ling, S.; Camp, J. S.; Slater, B.; Siepmann, J. I.; Sholl, D. S.; Snurr, R. Q. Advances, Updates, and Analytics for the Computation-Ready, Experimental Metal−Organic Framework Database: Core Mof 2019. *J. Chem. Eng. Data* **2019**, *64*, 5985−5998.
(5) Colón, Y. J.; Gómez-Gualdrón, D. A.; Snurr, R. Q. Topologically Guided, Automated Construction of Metal−Organic Frameworks and Their Evaluation for Energy-Related Applications. *Cryst. Growth Des.* **2017**, *17*, 5801−5810.
(6) Wilmer, C. E.; Leaf, M.; Lee, C. Y.; Farha, O. K.; Hauser, B. G.; Hupp, J. T.; Snurr, R. Q. Large-Scale Screening of Hypothetical Metal−Organic Frameworks. *Nat. Chem.* **2012**, *4*, 83−89.
(7) Gu, C.; Yu, Z.; Liu, J.; Sholl, D. S. Construction of an Anion-Pillared MOF Database and the Screening of MOFs Suitable for Xe/Kr Separation. *ACS Appl. Mater. Interfaces* **2021**, *13*, 11039−11049.
(8) Watanabe, T.; Sholl, D. S. Accelerating Applications of Metal−Organic Frameworks for Gas Adsorption and Separation by Computational Screening of Materials. *Langmuir* **2012**, *28*, 14114−14128.
(9) Tang, D.; Wu, Y.; Verploegh, R. J.; Sholl, D. S. Efficiently Exploring Adsorption Space to Identify Privileged Adsorbents for Chemical Separations of a Diverse Set of Molecules. *ChemSusChem* **2018**, *11*, 1567−1575.
(10) Gharagheizi, F.; Tang, D.; Sholl, D. S. Selecting Adsorbents to Separate Diverse near-Azeotropic Chemicals. *J. Phys. Chem. C* **2020**, *124*, 3664−3670.
(11) Qiao, Z.; Yan, Y.; Tang, Y.; Liang, H.; Jiang, J. Metal−Organic Frameworks for Xylene Separation: From Computational Screening to Machine Learning. *J. Phys. Chem. C* **2021**, *125*, 7839−7848.
(12) Bobbitt, N. S.; Snurr, R. Q. Molecular Modelling and Machine Learning for High-Throughput Screening of Metal-Organic Frameworks for Hydrogen Storage. *Mol. Simul.* **2019**, *45*, 1069−1081.
(13) Batra, R.; Song, L.; Ramprasad, R. Emerging Materials Intelligence Ecosystems Propelled by Machine Learning. *Nat. Rev. Mater.* **2021**, *6*, 655−678.
(14) Gurnani, R.; Yu, Z.; Kim, C.; Sholl, D. S.; Ramprasad, R. Interpretable Machine Learning-Based Predictions of Methane Uptake Isotherms in Metal−Organic Frameworks. *Chem. Mater.* **2021**, *33*, 3543−3552.
(15) Jiao, Y.; Li, Z.; Ma, Y.; Zhou, G.; Wang, S.; Lu, G. The Studies on Gas Adsorption Properties of MIL-53 Series MOFs Materials. *AIP Adv.* **2017**, *7*, No. 085009.
(16) Ramsahye, N. A.; Maurin, G.; Bourrelly, S.; Llewellyn, P.; Loiseau, T.; Ferey, G. Charge Distribution in Metal Organic Framework Materials: Transferability to a Preliminary Molecular Simulation Study of the CO_2 Adsorption in the MIL-53 (Al) System. *Phys. Chem. Chem. Phys.* **2007**, *9*, 1059−1063.
(17) Chokbunpiam, T.; Fritzsche, S.; Chmelik, C.; Caro, J.; Janke, W.; Hannongbua, S. Gate Opening Effect for Carbon Dioxide in ZIF-8 by Molecular Dynamics − Confirmed, but at High CO_2 Pressure. *Chem. Phys. Lett.* **2016**, *648*, 178−181.
(18) Dundar, E.; Chanut, N.; Formalik, F.; Boulet, P.; Llewellyn, P. L.; Kuchta, B. Modeling of Adsorption of CO_2 in the Deformed Pores of MIL-53(Al). *J. Mol. Model.* **2017**, *23*, No. 101.
(19) Salles, F.; Maurin, G.; Serre, C.; Llewellyn, P. L.; Knöfel, C.; Choi, H. J.; Filinchuk, Y.; Oliviero, L.; Vimont, A.; Long, J. R.; Férey, G. Multistep N_2 Breathing in the Metal−Organic Framework Co(1,4-Benzenedipyrazolate). *J. Am. Chem. Soc.* **2010**, *132*, 13782−13788.
(20) Witman, M.; Ling, S.; Jawahery, S.; Boyd, P. G.; Haranczyk, M.; Slater, B.; Smit, B. The Influence of Intrinsic Framework Flexibility on Adsorption in Nanoporous Materials. *J. Am. Chem. Soc.* **2017**, *139*, 5547−5557.
(21) Agrawal, M.; Sholl, D. S. Effects of Intrinsic Flexibility on Adsorption Properties of Metal−Organic Frameworks at Dilute and Nondilute Loadings. *ACS Appl. Mater. Interfaces* **2019**, *11*, 31060−31068.
(22) Jeffroy, M.; Nieto-Draghi, C.; Boutin, A. Molecular Simulation of Zeolite Flexibility. *Mol. Simul.* **2014**, *40*, 6−15.
(23) Tallury, S. S.; Pasquinelli, M. A. Molecular Dynamics Simulations of Polymers with Stiff Backbones Interacting with Single-Walled Carbon Nanotubes. *J. Phys. Chem. B* **2010**, *114*, 9349−9355.
(24) Vlugt, T. J. H.; Schenk, M. Influence of Framework Flexibility on the Adsorption Properties of Hydrocarbons in the Zeolite Silicalite. *J. Phys. Chem. B* **2002**, *106*, 12757−12763.
(25) García-Sánchez, A.; Dubbeldam, D.; Calero, S. Modeling Adsorption and Self-Diffusion of Methane in LTA Zeolites: The Influence of Framework Flexibility. *J. Phys. Chem. C* **2010**, *114*, 15068−15074.
(26) Anstine, D. M.; Tang, D.; Sholl, D. S.; Colina, C. M. Adsorption Space for Microporous Polymers with Diverse Adsorbate Species. *npj Comput. Mater.* **2021**, *7*, No. 53.
(27) Zhang, L.; Hu, Z.; Jiang, J. Sorption-Induced Structural Transition of Zeolitic Imidazolate Framework-8: A Hybrid Molecular Simulation Study. *J. Am. Chem. Soc.* **2013**, *135*, 3722−3728.
(28) Rogge, S. M. J.; Goeminne, R.; Demuynck, R.; Gutiérrez-Sevillano, J. J.; Vandenbrande, S.; Vanduyfhuys, L.; Waroquier, M.; Verstraelen, T.; Van Speybroeck, V. Modeling Gas Adsorption in Flexible Metal−Organic Frameworks Via Hybrid Monte Carlo/Molecular Dynamics Schemes. *Adv. Theory Simul.* **2019**, *2*, No. 1800177.
(29) Park, J.; Agrawal, M.; Sava Gallis, D. F.; Harvey, J. A.; Greathouse, J. A.; Sholl, D. S. Impact of Intrinsic Framework Flexibility for Selective Adsorption of Sarin in Non-Aqueous Solvents Using Metal−Organic Frameworks. *Phys. Chem. Chem. Phys.* **2020**, *22*, 6441−6448.
(30) Gee, J. A.; Sholl, D. S. Effect of Framework Flexibility on C_8 Aromatic Adsorption at High Loadings in Metal−Organic Frameworks. *J. Phys. Chem. C* **2016**, *120*, 370−376.
(31) Witman, M.; Wright, B.; Smit, B. Simulating Enhanced Methane Deliverable Capacity of Guest Responsive Pores in Intrinsically Flexible MOFs. *J. Phys. Chem. Lett.* **2019**, *10*, 5929−5934.
(32) Heinen, J.; Dubbeldam, D. On Flexible Force Fields for Metal-Organic Frameworks: Recent Developments and Future Prospects. *Wiley Interdiscip. Rev.: Comput. Mol. Sci.* **2018**, *8*, No. e1363.

(33) Rappe, A. K.; Casewit, C. J.; Colwell, K. S.; Goddard, W. A.; Skiff, W. M. UFF, a Full Periodic Table Force Field for Molecular Mechanics and Molecular Dynamics Simulations. *J. Am. Chem. Soc.* **1992**, *114*, 10024−10035.
(34) Coupry, D. E.; Addicoat, M. A.; Heine, T. Extension of the Universal Force Field for Metal−Organic Frameworks. *J. Chem. Theory Comput.* **2016**, *12*, 5215−5225.
(35) Fang, H.; Findley, J.; Muraro, G.; Ravikovitch, P. I.; Sholl, D. S. A Strong Test of Atomically Detailed Models of Molecular Adsorption in Zeolites Using Multilaboratory Experimental Data for CO_2 Adsorption in Ammonium ZSM-5. *J. Phys. Chem. Lett.* **2020**, *11*, 471−477.
(36) Nazarian, D.; Camp, J. S.; Chung, Y. G.; Snurr, R. Q.; Sholl, D. S. Large-Scale Refinement of Metal-Organic Framework Structures Using Density Functional Theory. *Chem. Mater.* **2017**, *29*, 2521−2528.
(37) Plimpton, S. Fast Parallel Algorithms for Short-Range Molecular Dynamics. *J. Comput. Phys.* **1995**, *117*, 1−19.
(38) Martyna, G. J.; Tobias, D. J.; Klein, M. L. Constant Pressure Molecular Dynamics Algorithms. *J. Chem. Phys.* **1994**, *101*, 4177−4189.
(39) Dubbeldam, D.; Calero, S.; Ellis, D. E.; Snurr, R. Q. Raspa: Molecular Simulation Software for Adsorption and Diffusion in Flexible Nanoporous Materials. *Mol. Simul.* **2016**, *42*, 81−101.
(40) Dubbeldam, D.; Torres-Knoop, A.; Walton, K. S. On the Inner Workings of Monte Carlo Codes. *Mol. Simul.* **2013**, *39*, 1253−1292.
(41) Wick, C. D.; Martin, M. G.; Siepmann, J. I. Transferable Potentials for Phase Equilibria. 4. United-Atom Description of Linear and Branched Alkenes and Alkylbenzenes. *J. Phys. Chem. B* **2000**, *104*, 8008−8016.
(42) Potoff, J. J.; Siepmann, J. I. Vapor−Liquid Equilibria of Mixtures Containing Alkanes, Carbon Dioxide, and Nitrogen. *AIChE J.* **2001**, *47*, 1676−1682.
(43) Hirschfelder, J. O.; Curtiss, C. F.; Bird, R. B. Molecular Theory of Gases and Liquids, In *Physical Chemistry*, Wiley, New York, 1964; Vol *165*, p 1280.
(44) Talu, O.; Myers, A. L. Reference Potentials for Adsorption of Helium, Argon, Methane, and Krypton in High-Silica Zeolites. *Colloids Surf., A* **2001**, *187-188*, 83−93.
(45) Manz, T. A.; Sholl, D. S. Chemically Meaningful Atomic Charges That Reproduce the Electrostatic Potential in Periodic and Nonperiodic Materials. *J. Chem. Theory Comput.* **2010**, *6*, 2455−2468.
(46) Manz, T. A.; Limas, N. G. Introducing DDEC6 Atomic Population Analysis: Part 1. Charge Partitioning Theory and Methodology. *RSC Adv.* **2016**, *6*, 47771−47801.
(47) Limas, N. G.; Manz, T. A. Introducing DDEC6 Atomic Population Analysis: Part 2. Computed Results for a Wide Range of Periodic and Nonperiodic Materials. *RSC Adv.* **2016**, *6*, 45727−45747.
(48) Frenkel, D.; Smit, B. Accelerating Monte Carlo Sampling. In *Understanding Molecular Simulation*; 2nd ed.,Frenkel, D.; Smit, B., Eds.; Academic Press, San Diego, 2002; pp 389−408.
(49) Cochran, W. The Effect of Anisotropic Thermal Vibration on the Atomic Scattering Factor. *Acta Crystallogr.* **1954**, *7*, 503−504.
(50) Pecharsky, V. K.; Zavalij, P. Y. Solving the Crystal Structure. In *Fundamentals of Powder Diffraction and Structural Characterization of Materials*; 2nd ed., Springer US, Boston, MA, 2009; pp 239−262.
(51) Pecharsky, V.; Zavalij, P.Y. *Fundamentals of Powder Diffraction and Structural Characterization of Materials*; 2nd ed., Springer, 2009; pp 239−262.
(52) Thyagarajan, R.; Sholl, D. S. A Database of Porous Rigid Amorphous Materials. *Chem. Mater.* **2020**, *32*, 8020−8033.
(53) Willems, T. F.; Rycroft, C. H.; Kazi, M.; Meza, J. C.; Haranczyk, M. Algorithms and Tools for High-Throughput Geometry-Based Analysis of Crystalline Porous Materials. *Microporous Mesoporous Mater.* **2012**, *149*, 134−141.
(54) Ongari, D.; Boyd, P. G.; Barthel, S.; Witman, M.; Haranczyk, M.; Smit, B. Accurate Characterization of the Pore Volume in Microporous Crystalline Materials. *Langmuir* **2017**, *33*, 14529−14538.
(55) Rogge, S. M. J.; Waroquier, M.; Van Speybroeck, V. Reliably Modeling the Mechanical Stability of Rigid and Flexible Metal−Organic Frameworks. *Acc. Chem. Res.* **2018**, *51*, 138−148.
(56) Moghadam, P. Z.; Rogge, S. M. J.; Li, A.; Chow, C.-M.; Wieme, J.; Moharrami, N.; Aragones-Anglada, M.; Conduit, G.; Gomez-Gualdron, D. A.; Van Speybroeck, V.; Fairen-Jimenez, D. Structure-Mechanical Stability Relations of Metal-Organic Frameworks Via Machine Learning. *Matter* **2019**, *1*, 219−234.
(57) Park, J.; Howe, J. D.; Sholl, D. S. How Reproducible Are Isotherm Measurements in Metal−Organic Frameworks? *Chem. Mater.* **2017**, *29*, 10487−10495.
(58) Agrawal, M.; Han, R.; Herath, D.; Sholl, D. S. Does Repeat Synthesis in Materials Chemistry Obey a Power Law? *Proc. Natl. Acad. Sci. U.S A.* **2020**, *117*, 877−882.
(59) Zang, J.; Nair, S.; Sholl, D. S. Osmotic Ensemble Methods for Predicting Adsorption-Induced Structural Transitions in Nanoporous Materials Using Molecular Simulations. *J. Chem. Phys.* **2011**, *134*, No. 184103.
(60) Coudert, F. X. The Osmotic Framework Adsorbed Solution Theory: Predicting Mixture Coadsorption in Flexible Nanoporous Materials. *Phys. Chem. Chem. Phys.* **2010**, *12*, 10904−10913.
(61) Waskom, M. L. Seaborn: Statistical Data Visualization. *J. Open Source Software.* **2021**, *6*, No. 3021.
(62) Breck, D. W. *Zeolite Molecular Sieves - Structure, Chemistry, and Use*, John Wiley & Sons, 1974; pp 593−725.
(63) Aguado, S.; Bergeret, G.; Daniel, C.; Farrusseng, D. Absolute Molecular Sieve Separation of Ethylene/Ethane Mixtures with Silver Zeolite A. *J. Am. Chem. Soc.* **2012**, *134*, 14635−14637.
(64) Matteucci, S.; Yampolskii, Y.; Freeman, B. D.; Pinnau, I. Transport of Gases and Vapors in Glassy and Rubbery Polymers. In *Materials Science of Membranes for Gas and Vapor Separation*; John Wiley & Sons, Ltd., 2006; pp 1−47.
(65) Gehre, M.; Guo, Z.; Rothenberg, G.; Tanase, S. Sustainable Separations of C_4-Hydrocarbons by Using Microporous Materials. *ChemSusChem* **2017**, *10*, 3947−3963.
(66) Walton, K. S.; Sholl, D. S. Predicting Multicomponent Adsorption: 50 Years of the Ideal Adsorbed Solution Theory. *AIChE J.* **2015**, *61*, 2757−2762.
(67) Ortiz, A. U.; Boutin, A.; Fuchs, A. H.; Coudert, F.-X. Anisotropic Elastic Properties of Flexible Metal-Organic Frameworks: How Soft Are Soft Porous Crystals? *Phys. Rev. Lett.* **2012**, *109*, 195502.
(68) Ortiz, A. U.; Boutin, A.; Fuchs, A. H.; Coudert, F.-X. Metal−Organic Frameworks with Wine-Rack Motif: What Determines Their Flexibility and Elastic Properties? *J. Chem. Phys.* **2013**, *138*, No. 174703.
(69) Bucior, B. J.; Bobbitt, N. S.; Islamoglu, T.; Goswami, S.; Gopalan, A.; Yildirim, T.; Farha, O. K.; Bagheri, N.; Snurr, R. Q. Energy-Based Descriptors to Rapidly Predict Hydrogen Storage in Metal−Organic Frameworks. *Mol. Syst. Des. Eng.* **2019**, *4*, 162−174.
(70) Yu, X.; Choi, S.; Tang, D.; Medford, A. J.; Sholl, D. S. Efficient Models for Predicting Temperature-Dependent Henry's Constants and Adsorption Selectivities for Diverse Collections of Molecules in Metal−Organic Frameworks. *J. Phys. Chem. C* **2021**, *125*, 18046−18057.

https://doi.org/10.1021/acsami.1c20583
ACS Appl. Mater. Interfaces 2021, 13, 61305−61315